

Measurement of optical trapping forces by use of the two-photon-excited fluorescence of microspheres

A. V. Kachynski, A. N. Kuzmin, H. E. Pudavar, D. S. Kaputa, A. N. Cartwright, and P. N. Prasad

The Institute for Lasers, Photonics, and Biophotonics, State University of New York at Buffalo, 458 Natural Sciences Complex, Buffalo, New York 14260-3000

Received April 30, 2003

A novel technique for the calibration of laser trapping systems that utilizes two-photon-excited fluorescence of commercial dye-stained microspheres has been demonstrated. The trapping forces as well as the trapping efficiency have been measured for various liquid environments and trapping depths. The trapping efficiency in water was found to decrease with an increase of trapping depths because of the enlargement of the trapping beam waist caused by aberrations of the optical system. © 2003 Optical Society of America

OCIS codes: 140.7010, 120.0120.

Laser trapping technology has been widely used in biology and physics for the measurement of the weak piconewton forces that are generally associated with interactions of particles on a micrometer or a nanometer scale. For these applications, accurate characterization of the trapping forces is of utmost importance, especially for particles that are close in size to the trapping wavelength. In this generalized Lorenz–Mie regime, there does not exist a well-defined theoretical force approximation, and it becomes essential to have a well-established experimental calibration technique. Many papers have been written on the application of laser tweezers, but few of them describe accurate force calibration measurements.^{1–9} In the research reported in most of those papers, trapping forces applied to polystyrene or glass spheres (or beads) were calibrated against viscous drag forces exerted by fluid flow. According to this method, the trapping forces are calculated by use of Stokes law on the basis of the escape velocity of the bead from the trap. For a typical setup, one experimentally arranges fluid flow by moving the microscope stage while a calibration particle is held stationary by the laser tweezer. In this case the value of the measured force is limited by the maximal velocity of the motorized or piezo-driven stage installed in the setup. In a similar setup, an optical trap containing a trapped particle is moved while the fluid-based sample remains stationary. To calibrate the trap, a sinusoidal displacement is applied to the trapped bead through a galvano mirror, and the escape velocity of the bead is calculated from a known frequency and a maximum amplitude of displacement.⁷ A drawback of this technique is that there is an inherent acceleration associated with the sinusoidal displacement that inevitably introduces error into the force calculations.

In this Letter we report a new measurement technique for determining the trapping forces of laser tweezers. Our technique capitalizes on a feature of our laser tweezers layout that permits us to achieve motion of a trapped particle in a circular trajectory. A constant angular velocity can be selected, and a tunable radius allows one to increase the speed of the particle incrementally about a circular path. The step increment of the trajectory radius is small compared with the diameter of rotation. Consequently,

the acceleration of the particle that occurs during its transition between two neighboring circular trajectories does not adversely affect the trapping force calculation. The radius of the circular path (when the particle escapes) corresponds to the particle's linear velocity, which one can use to calculate the trapping forces.

The two-photon-excited fluorescence (TPEF) of trapped commercial fluorescent beads generated by cw trapping beam excitation (previously observed and reported by Liu *et al.*¹⁰) was used for visual control and velocity measurement of the trapped particles. Both the circular trajectory and the TPEF properties of this new technique allowed us to measure the trapping parameters with high accuracy and reliability for trapping depths of 2–50 μm . By performing measurements with several liquid environments we obtained useful information about optical trapping forces for various viscosities and refractive indices.

Our dual-beam trapping system, described in Ref. 11, is based on an optical manipulator (Solar-TII, LM-2), a TEM₀₀ cw Nd:YAG laser (Coherent, Compass 1064-2000), and a modified inverted microscope (Nikon, TE-200). A galvanomirror pair was used to control the scanning beam and allowed us to move the beam in any X – Y trajectory (including circular) by the use of a manipulator software interface. An optical trap was formed by a 100 \times microscope objective (Nikon-Plane; NA, 1.3; 60% transmission at 1064 nm). The Z position of the trap was controlled by a piezo stage with an accuracy of 0.1 μm . A He–Ne laser was used as a pilot to display both the fixed and the scanning infrared (IR) traps if necessary. The laser manipulator provided the focusing of all four beams (two IR and two red) at one plane with a spot diameter at the $1/e^2$ level of ~ 1 μm . We estimated the IR beam profile by measuring the TPEF signal while scanning an immobilized 175-nm bead.

For the calibration experiments, commercial dye-stained polystyrene microbeads (Molecular Probes; refractive index, 1.56) with diameters of 0.175, 1, 2.5, and 6 μm were used. The liquid containing the beads was placed between a plain glass slide and a coverslip with a total depth chamber of ~ 100 μm . The high intensity of the cw IR light of the optical trap (0.1–20 MW/cm²) was able to produce two-photon

fluorescence (at ~ 580 nm) of the dye incorporated in the trapped beads. The experimental technique was as follows: Once the bead was successfully trapped, a circular trajectory of trap motion with a constant angular velocity was created through a software interface. The circle's radius was slowly increased, step by step, during trap rotation until the bead escaped. We determined that the bead escaped at a velocity that corresponded to the point at which the frictional force arising from the bead's motion exceeded the lateral trapping force of the optical trap. The minimum incremental step of radius increase was estimated to be ~ 14 nm, which is ~ 200 times less than the minimal experimentally determined value of the escaping radii. This technique permits a high degree of accuracy in force calibration measurements. Transverse trapping force F_{trap} was evaluated from the force balance equation for a rotating bead in the X - Y plane: $\mathbf{F}_{\text{trap}} + \mathbf{F}_f + \mathbf{F}_c = 0$, where \mathbf{F}_f and \mathbf{F}_c are friction and centrifugal forces, respectively [Fig. 1(a)]. Finally, using Stokes' law, we can show that

$$F_{\text{trap}} = 6\pi^2 d \nu r \left[(\beta \eta)^2 + \left(\frac{\pi d^2 \rho \nu}{16} \right)^2 \right]^{1/2}, \quad (1)$$

where d is the bead diameter, ν is the frequency of the trap rotation, r is the radius of the circle trajectory at which the bead escapes, η is the viscosity of the liquid environment, ρ is the density of the bead, and β is a surface effect coefficient that can be calculated from Faxen's formula.^{2,3} For typical parameters of beads used in optical trapping, the second term in Eq. (1) under the square root (centrifugal part) is negligibly small in comparison to the first term (friction part). Therefore the trapping force and the trapping efficiency Q can be calculated from the formulas

$$F_{\text{trap}} \approx 6\pi^2 d \nu r \beta \eta, \quad (2)$$

$$Q = \frac{F_{\text{trap}} c}{nP} = \frac{6\pi^2 d \nu r \beta \eta c}{nP}, \quad (3)$$

where c is the speed of light in vacuum, n is the refractive index of the environment, and P is the laser trapping power.

The frequency of trap rotation (angular velocity) ν in Eqs. (2) and (3) is a parameter of the optical tweezer layout, which should be calibrated separately before measurement of the trapping force. To calibrate the rotation frequency we immobilized a microsphere on the coverslip's surface and programmed the circular trajectory of the trapping beam to cross over it. The TPEF flashes excited by the IR beam during the motion of the beam over the bead were registered by a photomultiplier tube and a HP Infinium oscilloscope. The frequency of rotation was determined from the frequency of TPEF flashes on the oscilloscope.

The results of the trapping force measurements are presented in Figs. 1(b) and 2(a). The magnitude of the trapping force for the water environment is in accordance with other previously reported measurements.^{1,3,8,9} Furthermore, we found that the

dependence of the trapping force on laser power is nonlinear in the range 10–200 mW, and it can be approximated by a power dependence with an index of 0.8 for all diameters of beads used in the experiment [Fig. 1(b)]. The plot of trapping efficiency Q versus the bead diameter is also nonlinear and is close to that reported in Ref. 12.

To investigate trapping forces for media with different viscosities and refractive indices (as they pertain to trapping efficiency versus depth), we used water, dimethyl sulfoxide (DMSO), a DMSO–glycerol

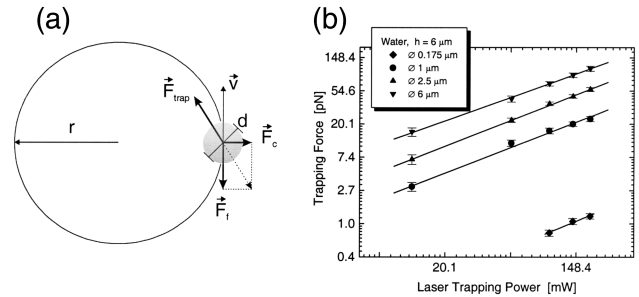


Fig. 1. Trapping forces: (a) diagram of transverse forces acting on a trapped bead during trap rotation in a liquid environment; (b) trapping forces versus trapping laser power measured for fluorescent beads of several diameters.

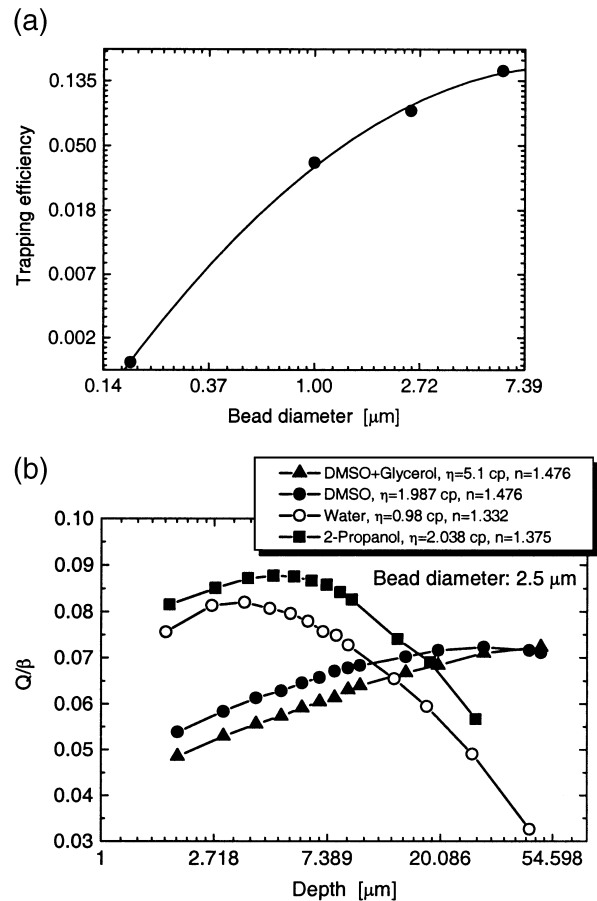
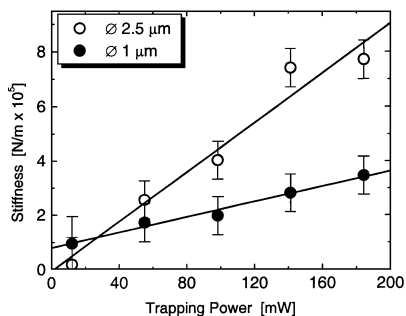


Fig. 2. Trapping efficiency: (a) its dependence on bead diameter, (b) dependence of Q/β on trap depth for various liquids; the viscosity of liquids is shown in centipoises (cp). The magnitude of the experimental error is comparable with the size of the symbols.

Table 1. Refractive Index and Viscosity of Liquids Used for Experiments^a

Solvent	Refractive Index	Viscosity (kg/m s ⁻¹ × 10 ⁻³)
Water	1.332	0.98
2-Propanol	1.375	2.038
DMSO	1.476	1.987
DMSO and glycerol	1.474	5.1

^aTemperature, 25 °C.Fig. 3. Trapping stiffness for $\varnothing 1$ and $\varnothing 2.5$ beads plotted versus trapping laser power.

mixture, and 2-propanol as environments for trapping 2.5- μm beads. The parameters of these liquids used for the calculation of trapping force and trapping efficiency are listed in Table 1. To analyze the results we plotted the experimentally determined trapping efficiency Q divided by coefficient β [see Eq. (3)] versus trapping depth [Fig. 2(b)]. For depths close to the thickness of the coverslip, an interfacial influence is clearly seen as an increase of Q/β . We found that, for depths less than 5 μm , the influence of the proximity of the boundary on the motion of the sphere cannot be accounted for by Faxen's formula. In contrast, for trapping depths of more than 5 μm this formula works quite well. The observed decrease of the trapping efficiency in water and 2-propanol environments for trapping depths deeper than ~ 5 μm most likely occurs because of spherical aberrations of the trapping beam's profile.³ The spherical aberrations could be caused by a refractive-index mismatch between the coverslip and the medium in which the particles are suspended.⁵ For the DMSO and DMSO-glycerol environments (where the refractive index of the medium is close to that of the glass coverslip), no essential aberration is expected. Correspondingly, no noticeable decrease in trapping efficiency with depth was observed.

To estimate the aberration of the trapping beam we measured the beam waist diameter at both the upper (medium-coverslip) and the lower (medium-slide) boundaries of the sample by using the CCD images of a focused IR beam. For the water environment the ratio of the beam diameters at the two boundaries was found to be approximately 2.4. If the diameter of the focused beam is assumed to change linearly with the depth of focusing, the dependence of the trapping force on beam diameter d_b can be evaluated from the data

in Fig. 2(b) as $F_{\text{trap}} \sim d_b^{-2}$. For the DMSO solvent, no difference in beam diameter was observed for the two locations, as expected because here there is a smaller refractive-index mismatch.

For estimation of the trapping stiffness of our laser tweezers we used the method of trapping dynamics described in Ref. 8. We measured the bead position as a function of the time during which the bead escaped from one stationary trap and was captured by another stationary trap separated by a distance $\sim d$. We arranged the trapping exchange by switching on the second beam milliseconds after switching off the first beam. The displacement of the particle during the motion from one trap to another was monitored by a photomultiplier tube signal generated from backscattering of the aiming He-Ne laser beam. The calibration measurements performed previously permit us to monitor the displacement with an accuracy of ~ 25 nm. The results of the trapping stiffness measurements are presented in Fig. 3. The calculated values of stiffness for our laser trapping system are close to those reported in Ref. 8.

In conclusion, we have proposed a novel, easy, and efficient technique for calibration of laser trapping systems by use of two-photon-excited fluorescence of commercially available dye-stained microspheres. Our experimental results reveal that the main reason for the decrease in trapping efficiency with increasing trapping depth in a water environment is the enlargement of the trapping beam waist created by aberrations.

This research was supported by the Directorate of Chemistry and Life Sciences of the U.S. Air Force Office of Scientific Research through Defense University Research Initiative on Nanotechnology grant F496200110358. A. N. Kuzmin's e-mail address is ankuzmin@acsu.buffalo.edu.

References

1. S. Sato, M. Ohyumi, H. Shibata, H. Hinaba, and Y. Ogawa, *Opt. Lett.* **16**, 282 (1991).
2. K. Svoboda and S. B. Block, *Annu. Rev. Biophys. Biomol. Struct.* **23**, 247 (1994).
3. W. H. Wright, G. J. Sonek, and M. W. Berns, *Appl. Opt.* **33**, 1735 (1994).
4. H. Felgner, O. Muller, and M. Schliwa, *Appl. Opt.* **34**, 977 (1995).
5. M. E. J. Friese, H. Rubinsztein-Dunlop, N. R. Heckenberg, and E. W. Dearden, *Appl. Opt.* **35**, 7112 (1996).
6. E. L. Florin, A. Pralle, E. H. K. Stelzer, and J. K. H. Horber, *Appl. Phys. A* **66**, S75 (1998).
7. S. Hénon, G. Lenormand, A. Richert, and F. Gallet, *Biophys. J.* **76**, 1145 (1999).
8. W. Singer, S. Bernet, N. Hecker, and M. Ritsch-Marte, *J. Mod. Opt.* **47**, 2921 (2000).
9. N. Malagnino, G. Pesce, A. Sasso, and E. Arimondo, *Opt. Commun.* **214**, 15 (2002).
10. Y. Liu, G. J. Sonek, M. W. Berns, K. Konig, and B. J. Tromberg, *Opt. Lett.* **20**, 2246 (1995).
11. P. N. Prasad, *Introduction to Biophotonics* (Wiley, New York, 2003).
12. W. H. Wright, G. J. Sonek, and M. W. Berns, *Appl. Phys. Lett.* **63**, 715 (1993).